processes

MDPI

Article

Study on Mechanical Behavior and Mechanism of Sandstone under the Coupling Effect of Water Content and Dynamic Load

Yang Chen [1,2], Ting Kang [3] and Chao Wu [4,*]

[1] School of Energy and Mining Engineering, China University of Mining and Technology (Beijing), Beijing 100083, China
[2] He Bei Hao Wei Xu Guang New Material Technology Co., Ltd., Handan 057350, China
[3] Shanghai Pudong Development Bank Co., Ltd., Taiyuan Zhenwu Road Sub-Branch, Handan 030000, China
[4] State Key Laboratory of Hydroscience and Hydraulic Engineering, Tsinghua University, Beijing 100084, China
* Correspondence: bqt1900101037@student.cumtb.edu.cn

Abstract: In the process of underground engineering construction, rock mass often faces the dual influence of dynamic load disturbance and groundwater, it is therefore essential to investigate the mechanical response of the rock mass under the coupling effect of dynamic load disturbance and water content. In this paper, dynamic load impact tests were carried out on sandstone with bullet velocities of 5 m/s, 10 m/s, and 15 m/s and water content of 0, 0.3, 0.6, and 0.9, and the mechanical behavior and mechanism response of water content to sandstone were investigated. The research findings indicate that this study has made significant contributions in quantifying the along grain and trans-grain fractures of microcracks. It has explored the influence of water content and dynamic loading on the strength mechanism of sandstone. It was discovered that the dynamic loading and water content significantly affect the ratio of along grain and trans-grain fractures, thereby influencing the dynamic behavior of sandstone. The findings suggest a negative association between rock strength and water content and that its peak strength rises as the bullet velocity rises. The fracture characteristics of rock are influenced by water content and bullet velocity. The sample's fracture degree increases with an increase in water content, its particle size distribution map is evident, and there is a positive relation between bullet velocity and fractal dimension. The energy conversion mechanism of the rock is influenced by the water content, as the bullet velocity increases, the absorbed energy density of the rock becomes higher. Furthermore, the correlation between the absorbed energy intensity and density and its fractal dimension is quantified. It is found that energy density and strength are positively correlated. The greater the fractal dimension, the higher the energy density absorbed.

Keywords: impact load; saturation degree; weakening of strength; crushing characteristics; energy conversion

Citation: Chen, Y.; Kang, T.; Wu, C. Study on Mechanical Behavior and Mechanism of Sandstone under the Coupling Effect of Water Content and Dynamic Load. *Processes* **2023**, *11*, 2318. https://doi.org/10.3390/pr11082318

Academic Editor: Jacopo Donnini

Received: 26 June 2023
Revised: 26 July 2023
Accepted: 28 July 2023
Published: 2 August 2023

1. Introduction

Under prolonged water immersion, the rock masses differ in their water content. The water content can greatly influence the energy dissipation mechanisms and crushing characteristics of rock, which has a significant impact on the safe construction of underground engineering. In addition, the rock mass is often subjected to dynamic load disturbance in underground engineering construction [1–4]. Therefore, water content and dynamic load disturbance serve a critical role in the way rock fragmentation characteristics and energy dissipation mechanism [5–8]. And thus, it is essential to investigate the energy dissipation mechanisms and strength properties of the rocks with various saturation degrees under impact for the safety of underground engineering.

The rock's mechanical behavior when exposed to different water contents has been extensively studied. Li examined the water content influencing the AE and mechanical

behavior of the sandstone under static load and discovered that water content is inversely proportional to rock strength and also significantly affects the AE behavior of rock [9]. Some scholars have also found that rock fracture mechanism varies as the water content rises [10–13]. Yin investigated the impacts of fracture and water content on the sandstone's mechanical behavior under uniaxial compression, found that various fracture lengths lead to different failure modes, and examined the mesoscopic degradation mechanisms in dry and saturated sandstones [14]. Kim performed tension and compression tests on sandstones of varying lithology and saturation to investigate the influence of saturation on Young's modulus, tensile strength and, and compressive strength came to the conclusion that the existence of water attenuated the dynamic parameters of the rocks [15]. Li examined the impact of water content on the sandstone's dynamic tensile strength and revealed that it has an inverse relationship with the sandstone's dynamic tensile strength, with marked differences in the degree of damage for sandstones with various water content [16]. Li studied the effect of different porosity on the dynamic load energy evolution of sandstone. It is found that water content significantly affects the mechanism of energy dissipation in sandstone, the impact of water content on the mechanism of energy dissipation in sandstones is studied from the aspect of fracture mechanics [17]. Zhao investigates the role of water content on the mechanism of energy evolution under mono-axial compression and finds that dry sandstone has a significantly higher energy release rate than saturated sandstone [18]. Wang conducted dynamic Brazilian splitting tests at different temperatures, water content, and loading rates and found that saturated rock samples had stronger rate dependence than dry rock samples, and temperature differences would affect the dynamic fracture mechanism of sandstone. Water content was found to be positively correlated with microwave heating of sandstone, and microwave treatment had a significant effect on sandstone water content [19,20]. Niu implemented dynamic impact tests on the red sandstone, which revealed that the crack propagation time was closely associated with the rock's water content, and the rate of crack extension reduced with rising water content. Furthermore, the experimental results were verified by numerical simulation [21]. Huang discovered that the saturation rate presents a critical strength value for the rock strength weakening [22]. Zhang examined the impact of water content on the sandstone's mechanical behavior at ultra-low temperatures and discovered that the failure pattern of the dry sandstone at ultra-low temperatures was markedly dissimilar to that of sandstone under saturated water conditions [23]. Matejunas researched the influence of water saturation on the damage properties and strength of concrete. Water saturation has been discovered to have a different influence on its strength and failure characteristics under static and dynamic loading conditions [24]. In a series of experiments to examine the pore distribution of sandstones in various saturated water, Zhou and Cai discovered that at identical water content, the sandstone tensile strength differed considerably [25–28]. Sandstone's fracture penetration rate clearly varies with varying water contents, based on Liu's study of the impact of water content on the damage features of the sandstone [29]. Natural and saturated sandstones were tested with tensile tests by Liu, who discovered that the crack propagation in sandstones began in the center [30]. Qi has carried out tensile tests on the ring sample with different saturation degrees and different temperatures, indicating that the water temperature is different, and the degree of sandstone rupture is different [31]. Corentin Noel studied the fracture toughness of sandstone under different water content conditions, and Stian Almenningen studied the effect of water on the transition of hydrate inside sandstone.

In summary, most research on rock mechanical behavior under different water content focuses on static load. Nevertheless, there are few studies on the mechanical behavior and fracture mechanism of sandstone under the coupling effect of different bullet velocities and different water contents. In this paper, dynamic compression tests were performed on sandstones with various water content and bullet velocity. The fractal size, strength, energy density–strength curves as well as energy density–fractal size of the sandstone were acquired, and the sandstone energy dissipation mechanism and strength features under the

coupling effect of various water content and elastic velocity were gained. In addition, the study has revealed the fragmentation characteristics and energy dissipation mechanism of sandstone under the coupled effects of different bullet velocities and water content. Additionally, it has made significant contributions by quantifying the fractures along and across grain boundaries at the microscale. The investigation has also explored the strength mechanism of sandstone under the coupled influence of water and dynamic loading.

2. Sample Treatment Process

Illustrated in Figure 1, the sample was taken in a mine in the Chinese province of Shaanxi. The XRD analysis revealed that the sample's main components were quartz (44.9%), clay minerals (28.3%), plagioclase (21.1%), siderite (2.3%), and calcite (1.3%). The collected rock samples were machined into cylindrical specimens with a height of 50 mm and a diameter of 50 mm.

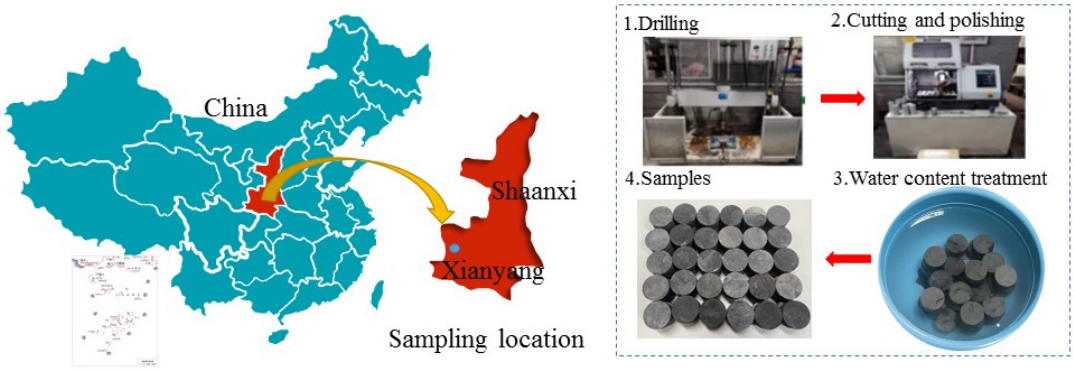

Figure 1. Rock specimen sampling and processing procedure.

Figure 2 shows the loading process of the test, at the same time, to maintain sample homogeneity as much as possible, when selecting samples for testing, it is important to avoid samples that exhibit prominent macroscopic cracks and voids. Before carrying out the test, we first tested the rock's natural water absorption properties. Figure 3 indicates that with the addition of soaking time to the rock sample, the rock saturation increases rapidly at first and then tends to be stable. This is due to the fact that rock samples have a finite water absorption rate, and when the rock sample is immersed in water at first, the fractures and pores in the rock open up and the water saturation of the rock initially rises rapidly. As the degree of saturation grows, the pores and cracks of the rock are gradually filled with free water. Therefore, the saturation of the rock sample tends to stabilize as the soaking time rises. In this paper, the relative saturation degree f is employed to depict the saturation of the rock samples. The following is the formula:

$$f = \frac{\omega_w}{\omega_s} = \frac{(m_w - m_d)/m_d}{(m_s - m_d)/m_d} \quad (1)$$

where f is the sample's saturation degree; ω_w is the moisture content after absorbing water; m_w is the mass after absorbing water; m_d is for natural mass; m_s is the mass at saturation. In this paper, as shown in Table 1, selected samples were immersed in water for 0, 0.6, 3, and 100 h, and the rocks with saturation degrees of 0, 0.3, 0.6, and 0.9 were prepared, respectively. In addition, we have to say that relative to the actual engineering, the bullet speed of 5 to 15 m/s is relatively low. To research the sandstone's energy conversion, failure and strength mechanisms under varying saturation degrees and bullet velocities, three dynamic loading tests were conducted on sandstone with different saturation degrees and different bullet velocities.

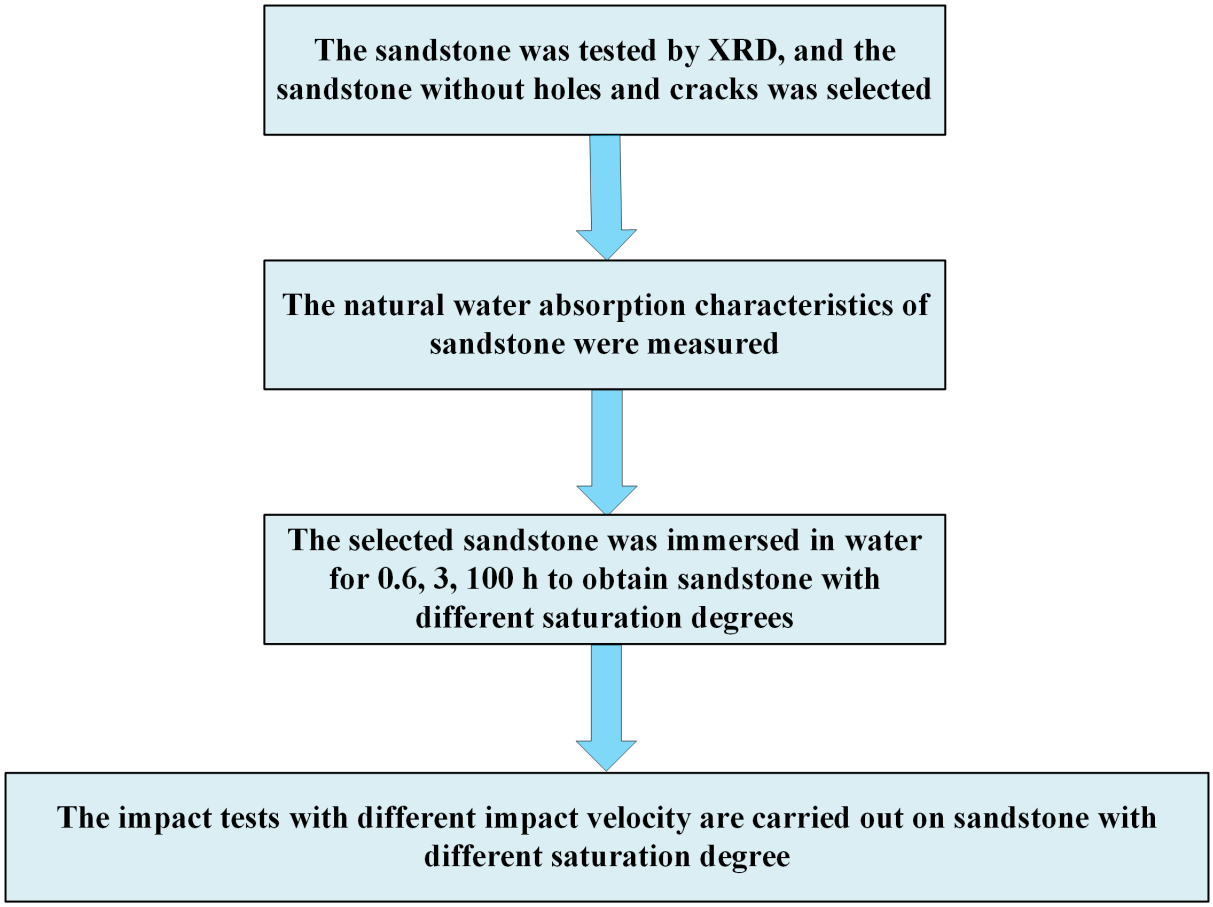

Figure 2. Testing procedure.

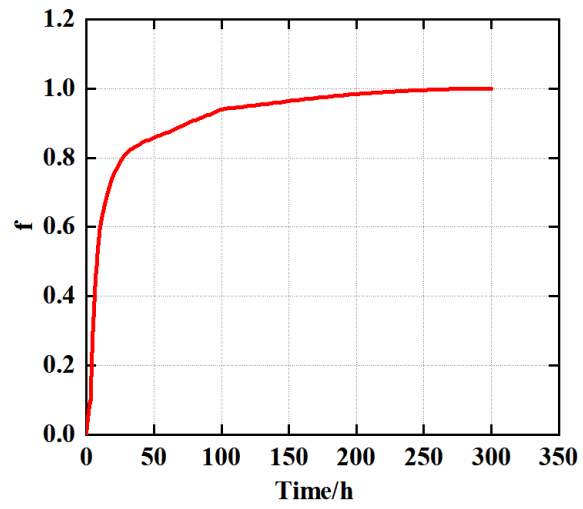

Figure 3. Water absorption curve of rock sample.

Table 1. Parameter table of sandstone.

Number.	Soaking Time /h	Natural Mass /g	The Mass after Absorbing Water /g	The Moisture Content after Absorbing Water /%	The Saturation Degree f
B-1	0	245.62	245.62	0	0
B-2	0	247.28	247.28	0	0
B-3	0	252.16	252.16	0	0
C-1	0.6	242.26	242.36	0.04	0.3
C-2	0.6	244.32	244.44	0.05	0.3
C-3	0.6	245.60	245.72	0.05	0.3
D-1	3	246.43	246.62	0.08	0.6
D-2	3	250.52	250.74	0.09	0.6
D-3	3	248.34	248.56	0.09	0.6
E-1	100	246.67	246.99	0.13	0.9
E-2	100	244.54	244.92	0.16	0.9
E-3	100	245.65	246.13	0.20	0.9

3. Test Equipment

Figure 4 and Table 2 display that the SHPB test system is adopted in this study. The system consists of a bullet launching system, a stress wave conduction system, an energy absorption system, and a data processing system, which can carry out dynamic impact tests on the sandstone with various impact velocities and saturation degrees. When performing this experiment, both ends of the sample were first wiped clean, and the ends of the sample were subsequently greased to minimize contact forces with the rod. After anchoring the sample, the bullet was inserted into the launching rod, fired, and the dynamic load compression test was completed. In addition, to decrease test error, the test was conducted on the bullet in the same position as much as possible. In accordance with the 1D stress wave theory, the sample's dynamic parameters can be acquired by the following formula [32–34], in addition, the strain (t) on the left is the strain of the sandstone sample, and the ε_I, ε_R, and ε_T on the right are the incident strain, reflected strain, and transmitted strain recorded by the improved SHPB.

$$\sigma(t) = \frac{A_e E_e}{2A_s}[\varepsilon_I(t) + \varepsilon_R(t) + \varepsilon_T(t)] \tag{2}$$

$$\varepsilon(t) = \frac{C_e}{L_s}\int_0^{\mathrm{t}}[\varepsilon_I(t) - \varepsilon_R(t) - \varepsilon_T(t)]\mathrm{dt} \tag{3}$$

$$\dot{\varepsilon}(t) = \frac{C_e}{L_s}[\varepsilon_I(t) - \varepsilon_R(t) - \varepsilon_T(t)] \tag{4}$$

where A_e, C_e and E_e denote the cross-sectional area, and wave velocity together with the elastic modulus of the bar, ε_I, ε_R, and ε_T represent the incident, reflected, and the transmitted strains, separately, A_s and L_s are the sample's cross-sectional area and length.

Table 2. Parameter of test system.

Equipment	Parameter of Apparatus
Bullet diameter	50 mm
Bullet length	45 mm
Bullet shape	Spindle bullet
Incident rod and transmission rod diameters	50 mm
Incident rod length	2500 mm
Transmission rod length	2500 mm
Total length of SHPB	8000 mm
SHPB Model number	ALT1000

Figure 4. SHPB and schematic diagram.

4. Test Results

4.1. Stress–Strain Curve

Figure 5 shows the voltage and time evolution curve of typical sandstone. According to the figure, the author selects three kinds of waves to calculate the stress–strain of sandstone. Rock properties undergo changes with varying water content, and the stress–strain curve is a fundamental tool for studying these properties. In this study, stress–strain curves were plotted for rocks subjected to different water content and impact velocities, as depicted in Figure 6. The stress–strain curve exhibits three distinct stages: elastic, plastic, and post-peak. Analysis of Figure 6 reveals a notable influence of water content on the strength of the rock specimens. As water content increases, the peak value of the stress–strain curve decreases. This phenomenon can be attributed to the enhanced interconnectivity of weaker pores and fractures within the rock formation facilitated by increased water content, resulting in a reduction in the peak value of the stress–strain curve.

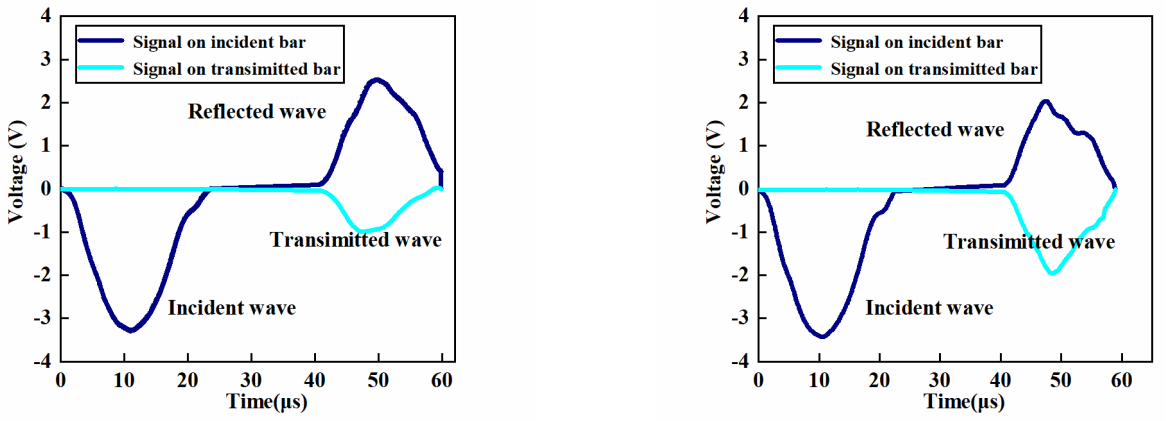

(**a**) f = 0, V = 5 m/s (**b**) f = 0.9, V = 5 m/s

Figure 5. Voltage and time evolution curve of typical sandstone.

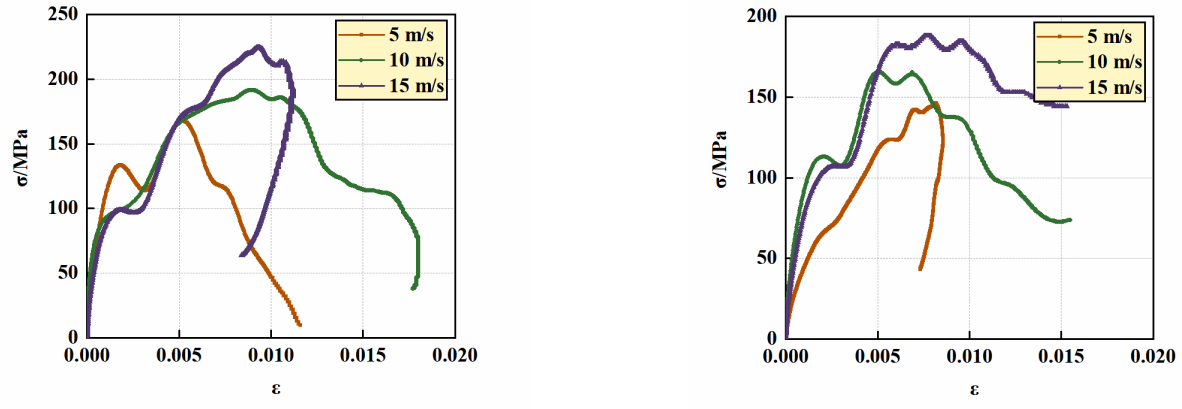

f = 0 f = 0.3

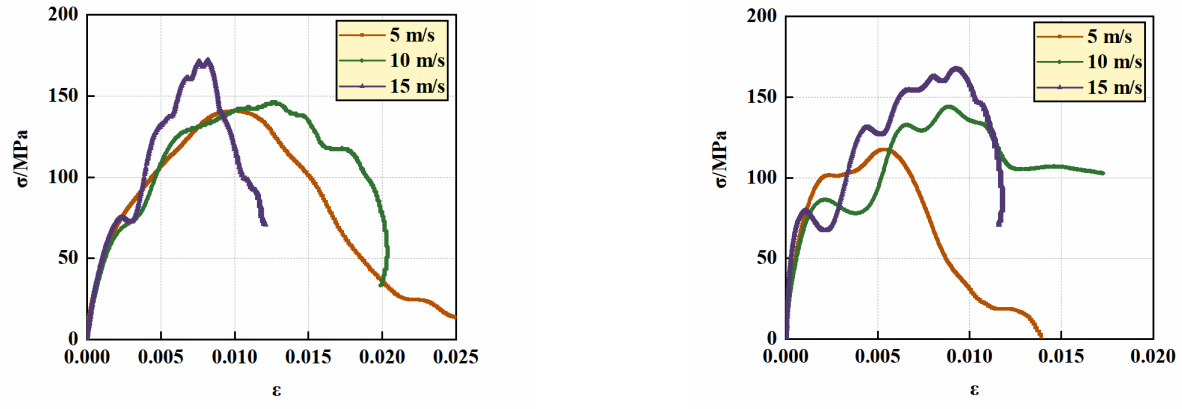

f = 0.6 f = 0.9

Figure 6. *Cont.*

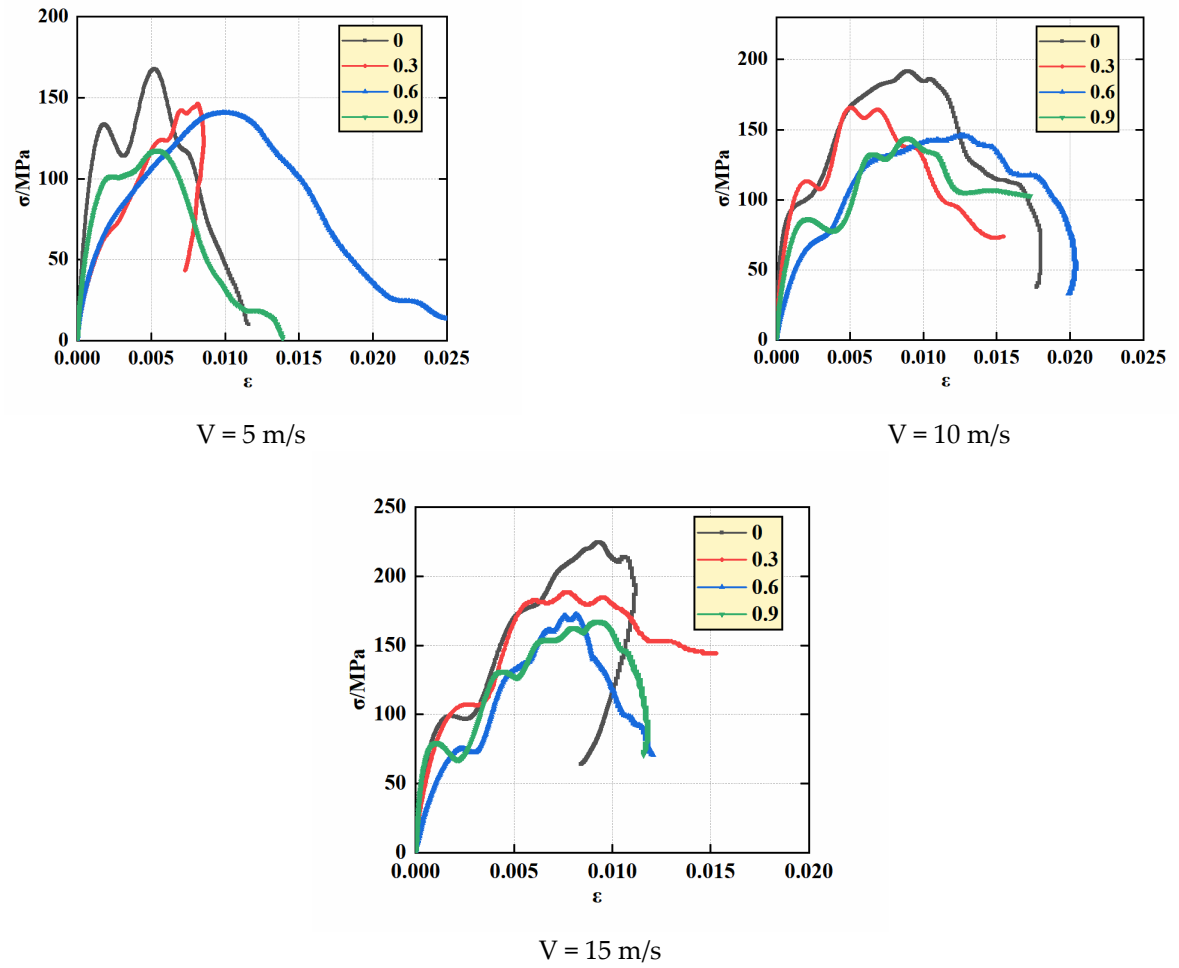

Figure 6. Stress–strain curves of sandstone with different water content and impact velocity.

4.2. Rock Strength Mechanism

After absorbing water, the particles inside the rock will interact with water in a variety of ways and resulting in a macroscopic difference in rock strength. Therefore, research into the strength characteristics of water-bearing rocks has always become a hot topic in rock mechanics. Many scholars have studied the strength characteristics of water-bearing rocks and found that in most cases, water will weaken the strength of rocks, while some scholars have discovered that water can enhance the strength of rocks [35–37]. However, there are few studies on the dynamic strength of the rock at various impact velocities and degrees of saturation. Thus, dynamic impact tests with diverse impact velocities were implemented on rocks with different saturation degrees to further investigated the mechanism of impact of impact velocity and saturation degree on rock strength. The rock's dynamic strength under different saturation degrees and impact velocities is depicted in Figure 7 and Table 3. As for the cloud map, the color of the cloud image represents the different peak strengths of the sandstone, and the corresponding relationship between the color and the peak strength of the sandstone can be seen in the label on the right. It can be seen from the cloud map that the peak strength of sandstone is proportional to the impact velocity and saturation degree. The rock's dynamic strength reduces as the saturation of water rises. For example, when the saturation of the rock is 0, 0.3, and 0.6, the rock's dynamic strength is 167.25 MPa, 146.13 MPa, and 139.89 MPa, respectively. This suggests that water exerts a strong effect on the strength of the sandstone. Furthermore, the rock's dynamic strength enhances with the rise in impact velocity. As an example, the rock's dynamic strength is 167.25, 191.62, and 224.62 MPa for impact velocities of 5 m/s, 10 m/s, and 15 m/s, separately.

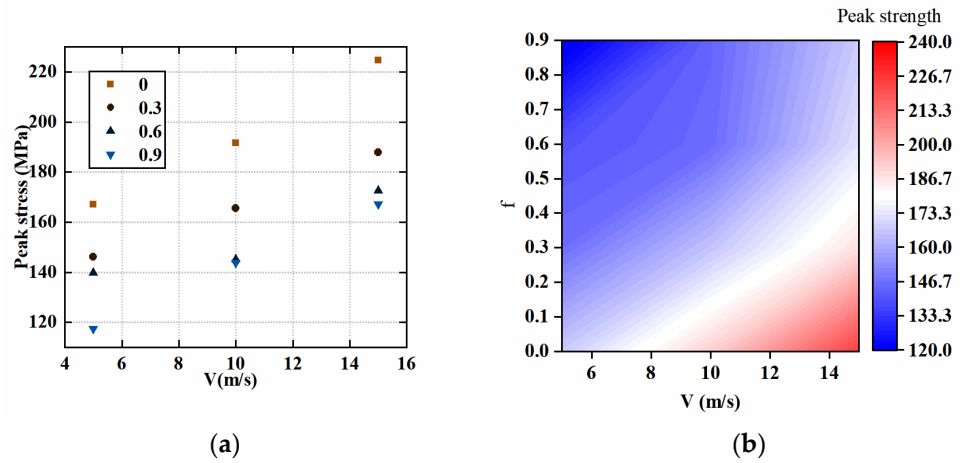

Figure 7. Peak stress characteristics of sandstone with different water content and impact velocity. (**a**) scatter plot; (**b**) cloud map.

Table 3. Strength of different saturated sandstones.

Bullet Velocity (m/s)	Satisfied Degree of Water (%)	Peak Strength /MPa
5	0	167.25
10	0	191.62
15	0	224.62
5	0.3	146.13
10	0.3	165.49
15	0.3	187.92
5	0.6	139.89
10	0.6	145.26
15	0.6	172.71
5	0.9	117.45
10	0.9	143.86
15	0.9	167.24

For further research into the mechanism of water weakening on the strength of rock, the author discusses the reaction mechanism of water in the rock. As we can see in Figure 8, numerous naturally hydrophilic minerals can be found throughout the rock's interior, and they all interact with water in different ways. These substances transform into different substances when they interact with water, such as montmorillonite reacting with water chemically as:

$$AI_4SI_4O_{10}(OH)_2 + nH_2O \rightarrow AI_4SI_4O_{10}(OH)_2 \cdot nH_2O$$

When a rock is immersed in water, the cracks and pores inside it will be filled with water, which will create surface tension in the pores. This tension will also make the rock less strong. This is because surface tension is the result of mutual attraction between water molecules, causing the water film to exhibit a membranous structure. This surface tension creates an internal positive pressure within the water film, attempting to reduce its surface area. When rocks are subjected to external stress, the surface tension of the water film induces internal tensile stress, thereby reducing the effective stress of the rock and weakening its strength. Additionally, the capillary force formed by rock particles and water is an important factor affecting rock strength. In Figure 8, when the rock is saturated with water, hydrophilic material inside the rock will expand in volume after encountering water, and its capillary force will decrease. So, its strength will also be reduced.

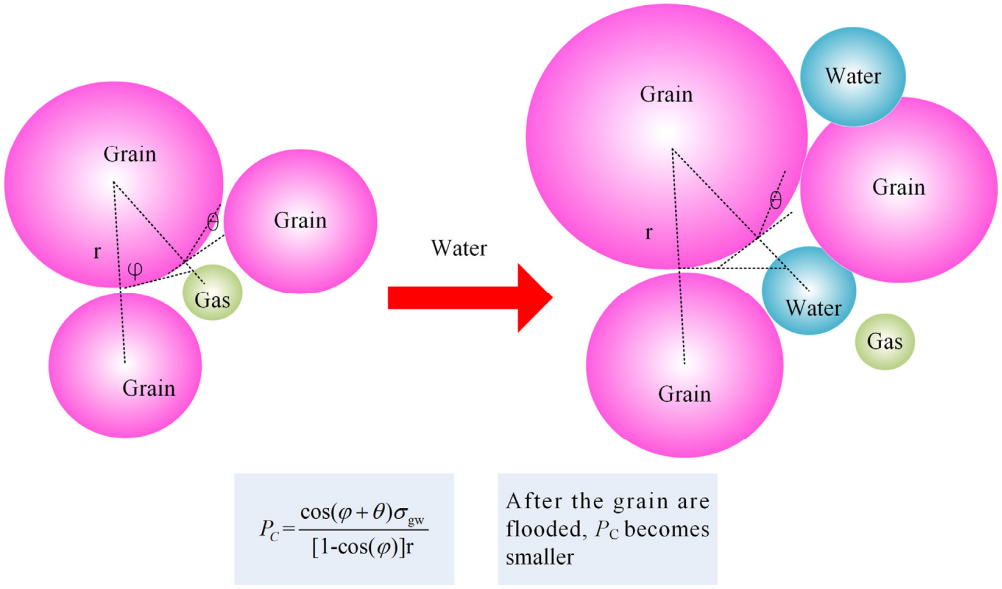

Figure 8. Water-bearing fracture mechanism of the sample.

The presence of free water in rock formations has a decelerating effect on crack propagation at higher velocities. Figure 9 illustrates three primary factors contributing to this phenomenon: σ_1, induced stress from the meniscus effect. At lower bullet velocities, as shown in Figure 9, free water is unable to reach the crack tip, resulting in the formation of σ_1. σ_2 represents stress caused by the Stefan effect, while σ_3 represents stress arising from Newtonian internal friction. At higher bullet velocities, the inertia of free water becomes a significant contributor to the formation of σ_3. Moreover, the movement of water molecules generates a tensile stress σ_4 at the crack tip, denoted as h. Notably, at higher impact velocities, the effects of σ_3 and σ_4 become more pronounced.

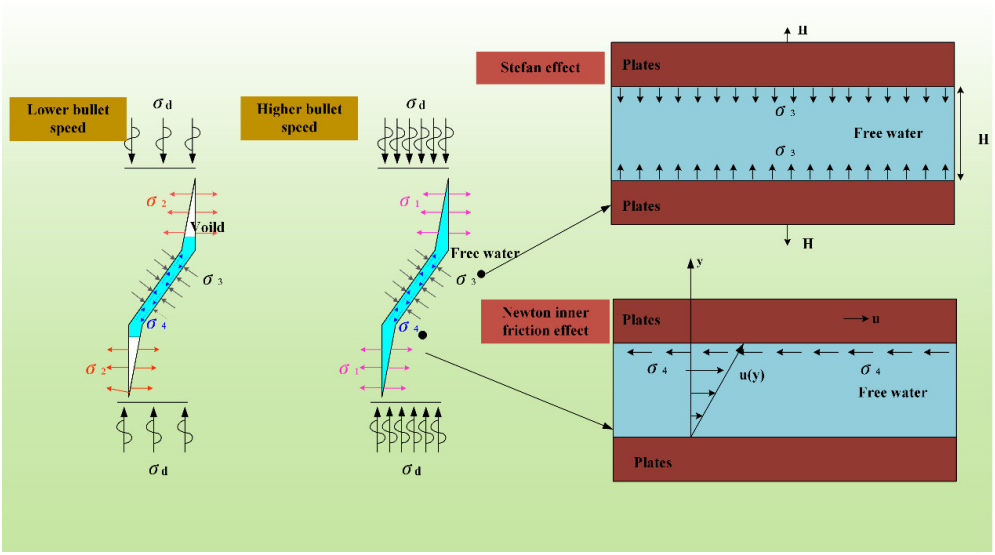

Figure 9. Mechanisms of strength effects in sandstone under different impact velocities.

The meniscus effect (σ_1) is the phenomenon where the unique arrangement and interaction of water molecules in crescent-shaped pores result in the generation of stresses and strains within the rock. This effect has been extensively studied in rock mechanics and plays a significant role in understanding stress and deformation in rocks in practical engineering and geological environments.

The Stefan effect (σ_2) refers to the phenomenon where temperature gradients or changes in a water-containing rock induce internal stresses due to the phase transition of water. The manifestation of the Stefan effect depends on the water content, rate of temperature change, and physical properties of the rock.

The Newtonian inner friction effect (σ_3) refers to the stresses generated by the frictional interaction between water molecules and rock particles during parallel relative motion in the presence of water. The Newtonian inner friction effect is particularly important in rock mechanics, especially in lubricated rocks or in the presence of water-filled fractures.

Tensile stress at the crack tip (σ_4) refers to the tensile stress state at the tip of a crack. When cracks exist in rocks or other materials, the crack tip becomes a region of stress concentration due to the abrupt change in the stress field at the tip.

4.3. Rock Size Distribution

Water will cause a chemical reaction with the material inside the rock mass once it has been immersed in the water. Additionally, because of the different degrees of water saturation, the degree of the chemical reaction varies as well. This effect will weaken the strength of the rock. Different impact velocities will have different effects on rock properties. Under the same load, rocks with different strengths have different degrees of damage. Therefore, it is essential to quantitatively analyze sandstone fragments with varying water contents to examine their fractal character. The fractal dimension calculation process is as follows:

$$\frac{M_x}{M_t} = \left(\frac{d_x}{d_m}\right)^{3-D} \tag{5}$$

In the equation, d_x represents the size of an individual particle, d_m refers to the maximum size of the sample fragment, M_t represents the total mass of the sample after crushing, M_x denotes the cumulative mass of the fragments with sizes smaller than d_x, and D represents the fractal dimension of the fragment size distribution in the sample.

$$\lg\left(\frac{M_x}{M_t}\right) = (3-D)\lg\left(\frac{d_x}{d_m}\right) \tag{6}$$

Figure 10 is the fractal process of the specimen. The distribution of mass and frequency is depicted in Figure 11. The figure illustrates that the water content will have a major influence on the mass frequency distribution diagram of rocks. Furthermore, as can be observed from the figure, the bullet velocity significantly affects the mass frequency distribution of the rock. The mass frequency profile is at the top when the bullet is traveling at 15 m/s. Figure 12 is a schematic diagram of the fractal dimension. From the figure, it is clear that with a rise in water content, the fractal dimension increases. For instance, when the velocity of the bullet is 15 m/s, D is 2.07 and the water content is 0. When the water content is 0.9, D is 2.17. Bullet velocity also significantly affects the fractal dimension. There is a positive association between fractal size and bullet velocity. The water content influences the distribution of particle size in the rocks considerably. There is a positive relation between the rock's fractal dimension and water content.

Figure 10. Fractal process of the specimen.

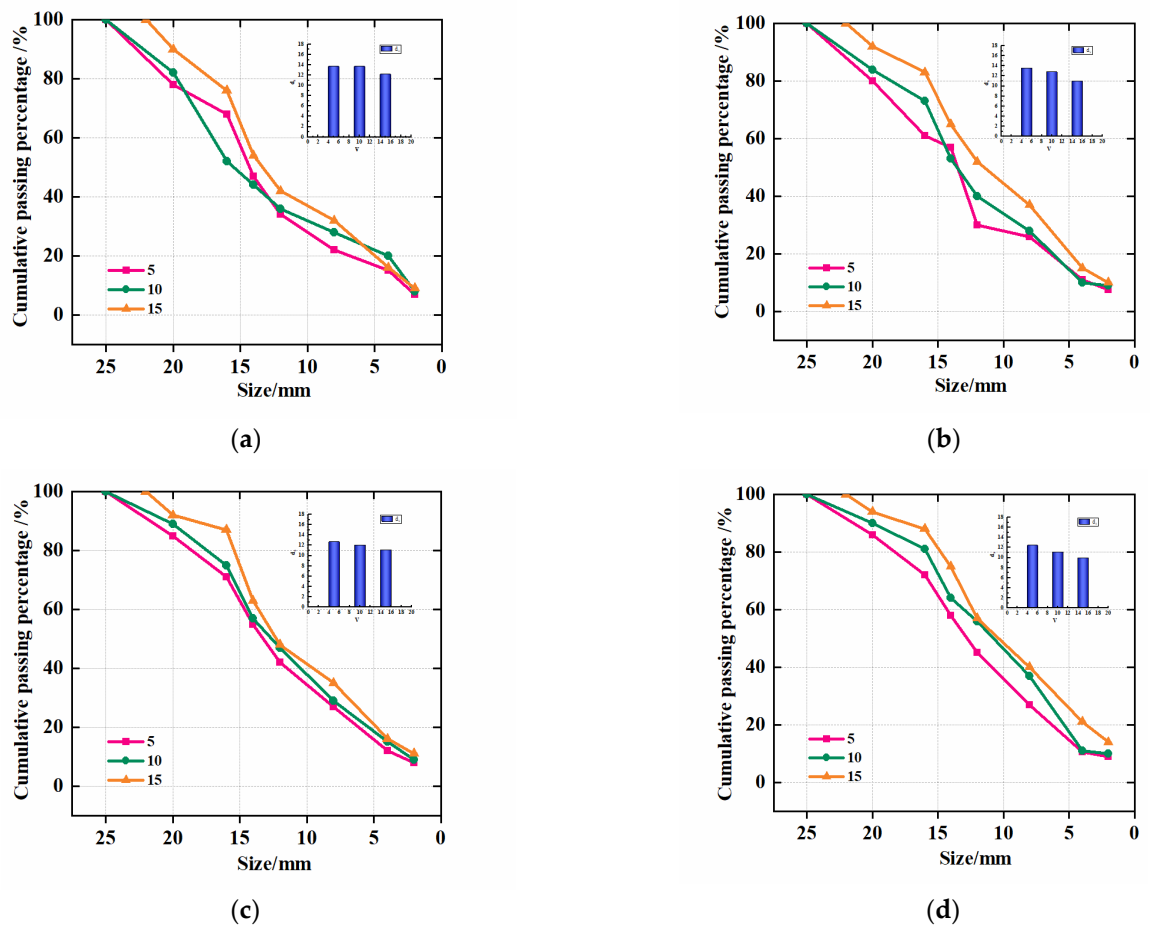

Figure 11. Sample size distribution characteristics. (**a**) f = 0; (**b**) f = 0.3; (**c**) f = 0.6; (**d**) f = 0.9.

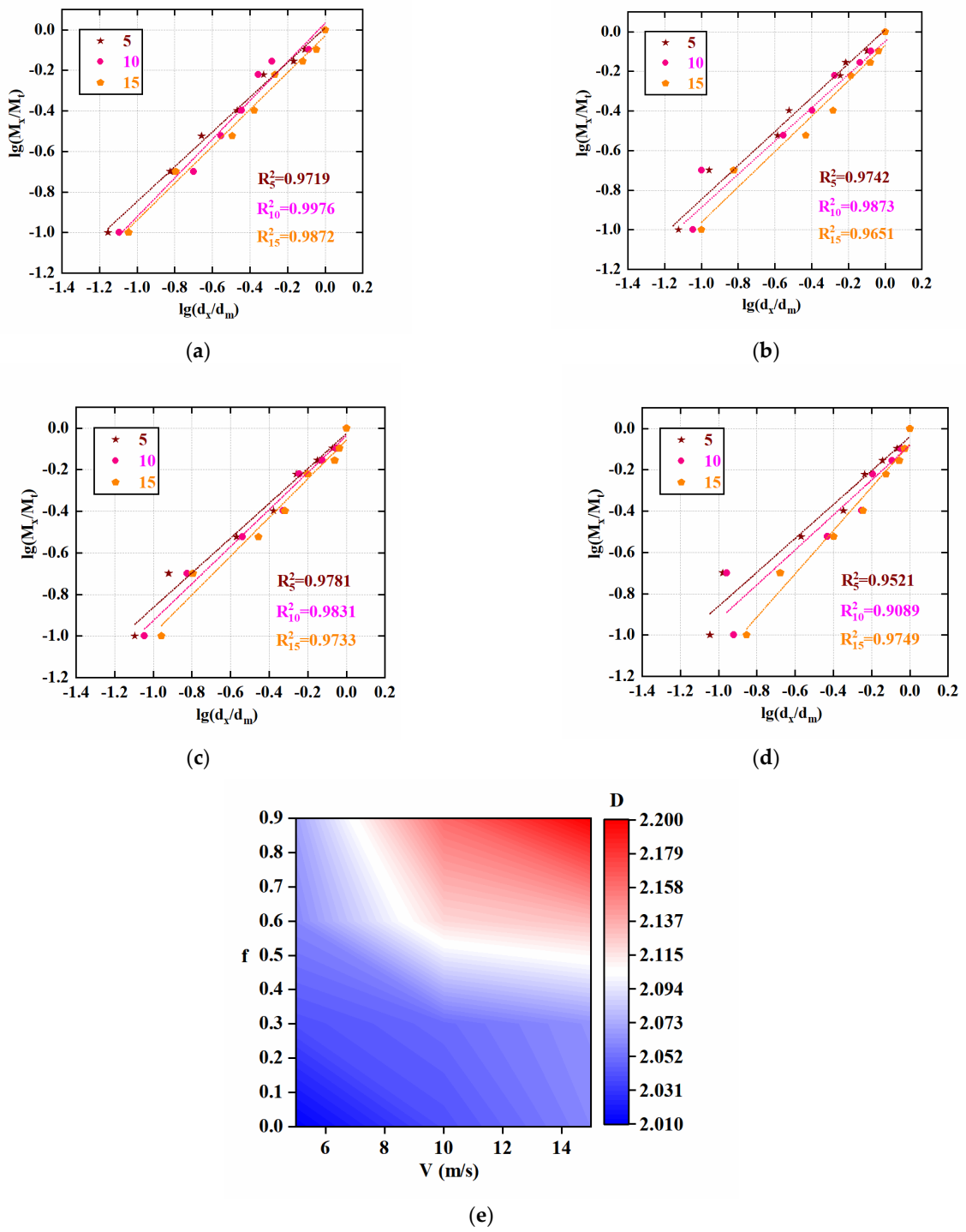

Figure 12. Fractal dimension characteristics of samples. (**a**) f = 0; (**b**) f = 0.3; (**c**) f = 0.6; (**d**) f = 0.9; (**e**) fractal dimension cloud map.

4.4. Rock Energy Dissipation Mechanism

Different water contents inevitably cause changes in the composition of rocks. Therefore, the internal energy conversion must be affected by the water content. Therefore, the following formula is adopted in this paper [38–40]:

$$W_I = \frac{A_e C_e}{E_e} \int \sigma_I^2(t) \mathrm{d}t \tag{7}$$

$$W_R = \frac{A_e C_e}{E_e} \int \sigma_R^2(t) \mathrm{dt} \tag{8}$$

$$W_T = \frac{A_e C_e}{E_e} \int \sigma_T^2(t) \mathrm{dt} \tag{9}$$

$$W_S = W_I - W_R - W_T \tag{10}$$

$$\varsigma = \frac{W_S}{V} \tag{11}$$

In formula: W_I, W_R, and W_T is the incident, reflective, and transmitted energy, W_S is energy, ς is energy consumption density.

Calculations are made to determine the energy value and energy proportion of different water-content sandstones to explore the impacts of water content and bullet velocity on the energy conversion mechanism of sandstone. Figure 13 and Table 4 show energy values for the sandstone with diverse water content. The energy conversion of sandstone is significantly influenced by bullet velocity. Each sandstone energy value rises in line with an increase in bullet velocity. In addition, Figure 14 shows the sandstone's energy evolution curve. The figure shows the energy conversion mechanism of rocks with significant water content. According to this figure, the water content affects little the incident energy of the sandstone, while it strongly affects other energy values. In addition, the incident energy of sandstone is significantly different with different bullet velocities. Therefore, the author studies the relationship between reflected, absorbed, and transmitted energy of the sandstone under the influence of varying incident energy from the point of view of incident energy. Figure 15 presents that with rising incident energy, the reflected, absorbed, and transmitted energy of the sandstone also increases. Moreover, energy dissipation density is typically employed to describe the character of energy dissipation. Hence, this paper explores the evolution of the energy dissipation density of sandstone under water content and impact velocity. The figure shows that the water content has little influence on energy dissipation density, whereas bullet velocity has a significant influence on energy dissipation density. The velocity of the bullet is positively associated with the energy dissipation density. Moreover, the bullet's velocity is proportional to the rock's incident energy. This may be due to the fact that as the bullet's velocity increases, the incident strain of the rock also increases, and thus its incident energy increases.

Table 4. Energy of sandstone under different degrees of saturation.

Bullet Velocity m/s	f	W_I/J	W_R/J	W_T/J	W_S/J
5	0	198.24	44.12	62.9296	91.1904
10	0	376.24	94.67	119.7868	161.7832
15	0	587.98	154.78	168.609	264.591
5	0.3	204.86	52.24	62.4816	90.1384
10	0.3	396.67	99.28	134.7553	162.6347
15	0.3	610.98	167.45	168.589	274.941
5	0.6	189.24	46.28	63.4792	79.4808
10	0.6	410.56	109.87	120.0436	180.6464
15	0.6	606.24	167.24	184.3792	254.6208
5	0.9	210.78	55.24	73.3358	82.2042
10	0.9	398.89	102.54	144.7718	151.5782
15	0.9	589.23	178.26	163.4934	247.4766

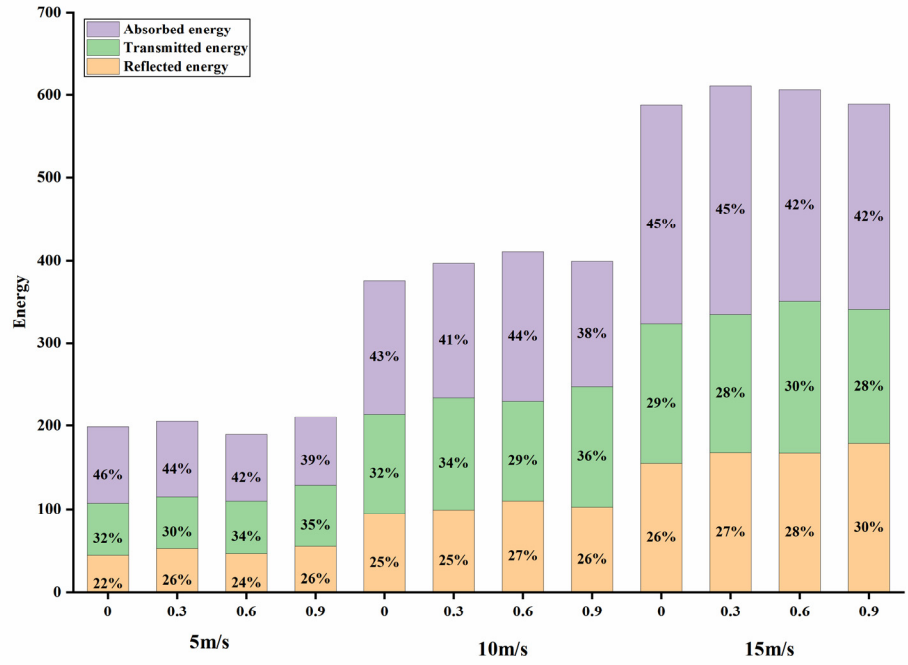

Figure 13. Energy proportion.

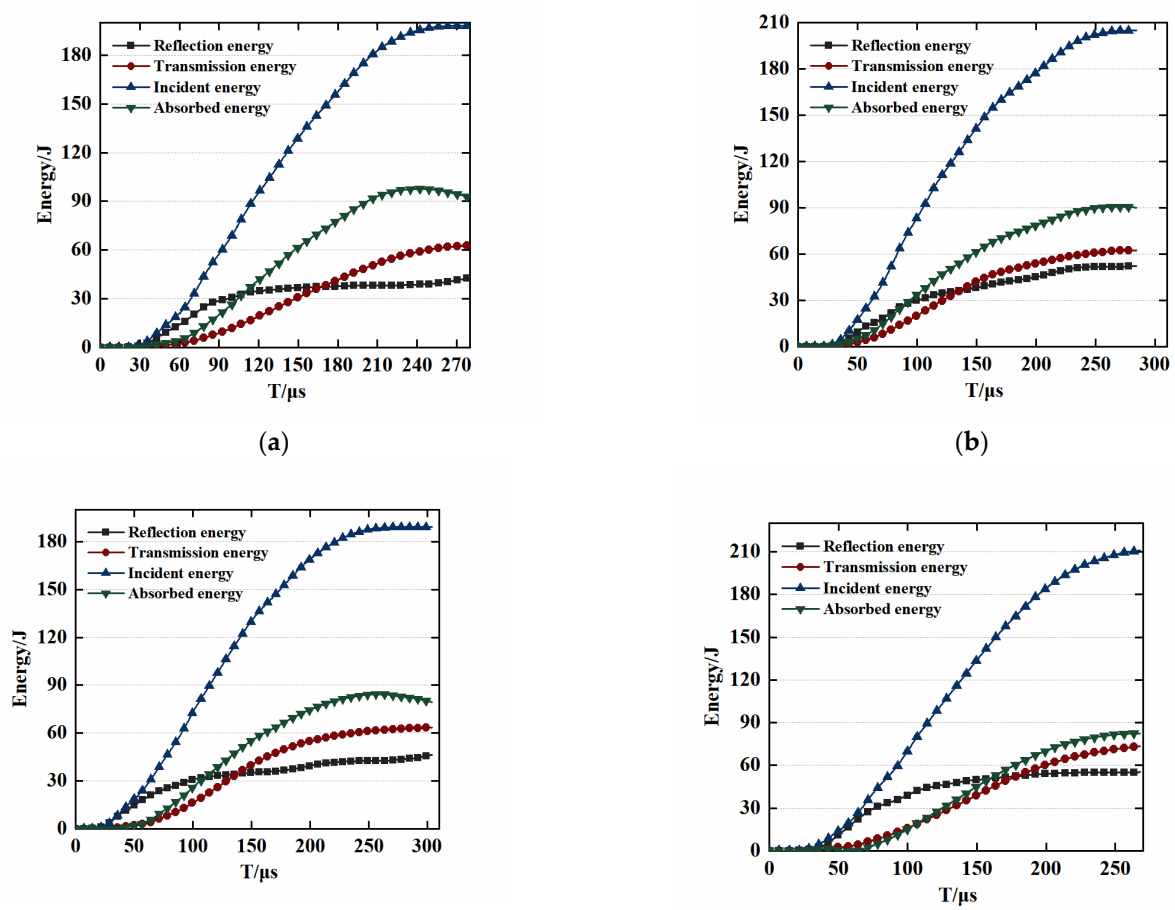

Figure 14. Whole energy evolution. (**a**) f = 0; (**b**) f = 0.3; (**c**) f = 0.6; (**d**) f = 0.9.

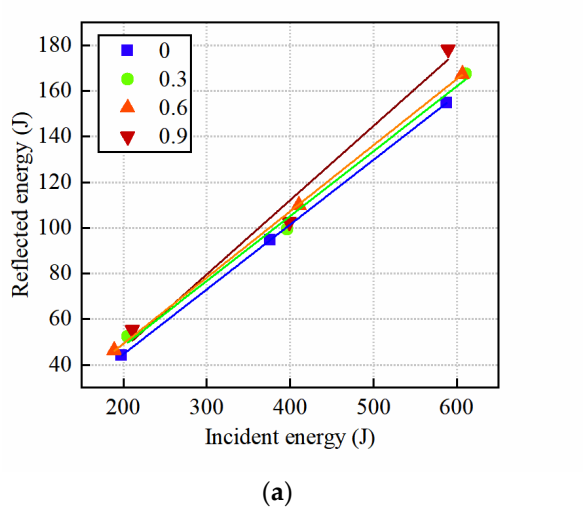

(**a**)

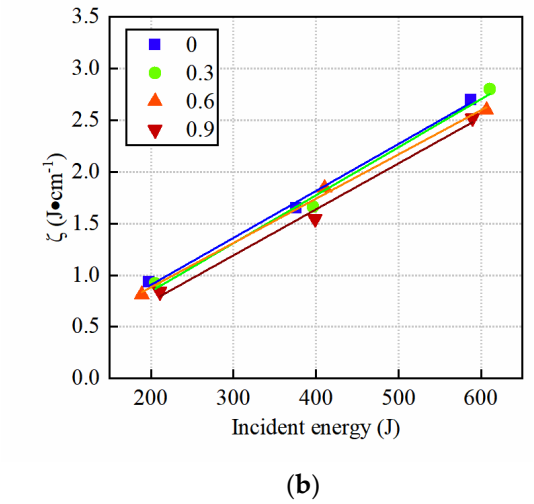

(**b**)

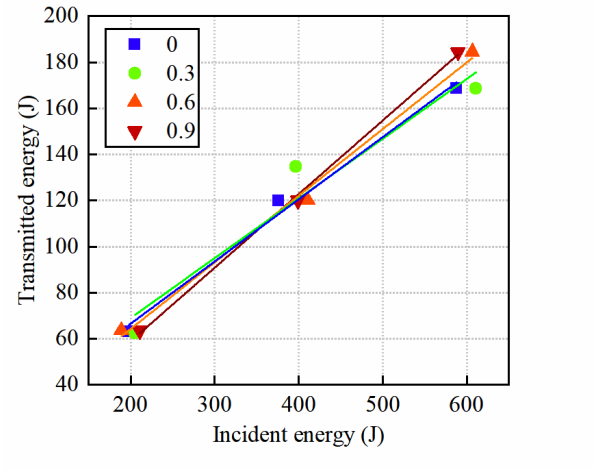

(**c**)

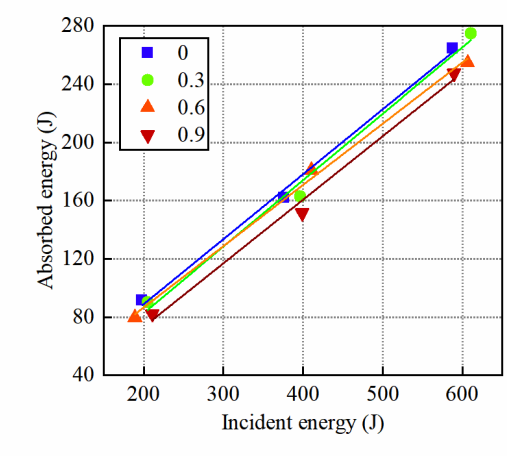

(**d**)

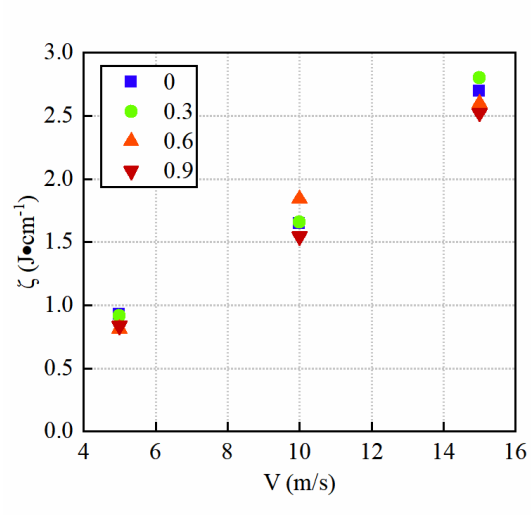

(**e**)

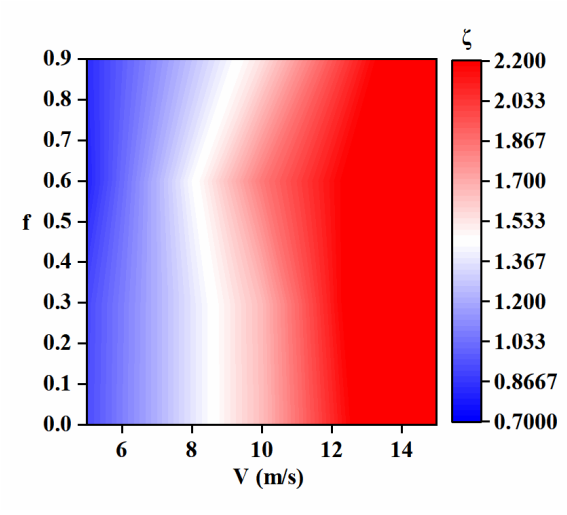

(**f**)

Figure 15. Evolution characteristics of incident energy–energy. (**a**) Incident energy—Reflected energy; (**b**) Incident energy—Energy consumption density; (**c**) Incident energy—transmitted energy; (**d**) Incident energy—absorbed energy; (**e**) Bullet velocity—Energy dissipation density; (**f**) Bullet velocity—Energy dissipation density cloud picture.

4.5. Relationship between Energy Consumption Density and Dynamic Intensity

Numerous studies demonstrate a significant correlation between rock's dynamic strength and energy dissipation density. As a result, this paper investigates the association between the sandstone's energy dissipation density and its dynamic strength under different water content and bullet velocity. Figure 16 illustrates the correlation between sandstone's dynamic strength and energy dissipation density for a variety of elastic velocities and water content. As shown in the figure, the relation between dynamic strength and energy dissipation density is basically positive. With a saturation degree of 0 and impact velocity of 5 m/s, the energy dissipation density of sandstone is 1.06 and its dynamic strength is 167.25 MPa. With a saturation degree of 0 and impact velocity of 10 m/s, the dynamic strength of sandstone is 1.62, and its dynamic strength is 191.62 MPa. The findings suggest that the dynamic intensity evolution and energy dissipation density are basically consistent. In practical engineering, the rock's dynamic strength will unavoidably increase when the density of energy dissipation within the rock is high.

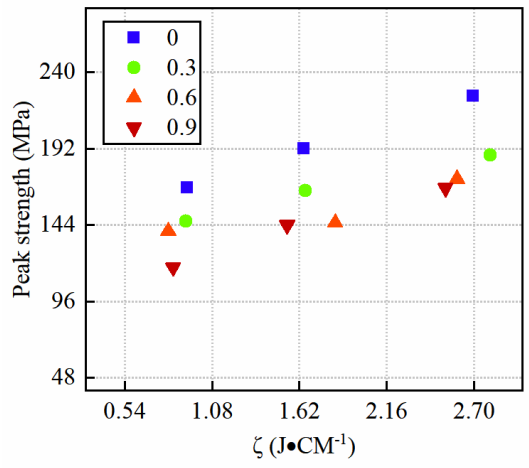

Figure 16. Correlation between the energy consumption density and dynamic strength of samples.

4.6. Relationship between Energy Consumption Density and Fractal Dimension

Energy consumption plays a critical role in underground construction, particularly in processes involving rock breakers or blasting. Rock breakers are mechanical devices used to fragment rock mass in underground construction. The energy consumption of rock breakers directly impacts their efficiency and performance. While higher energy consumption often leads to more effective rock fragmentation, excessive energy usage can result in unnecessary vibrations, noise, and equipment wear. Hence, finding the optimal balance between energy input and desired rock fragmentation is crucial for maximizing efficiency and minimizing drawbacks. Blasting, a widely employed technique for rock excavation, primarily affects drilling and explosive charging processes. Drilling necessitates energy for creating boreholes, while explosive charging involves energy consumption for handling and placing explosives. Controlling the energy input in blasting is vital to achieve desired results without wasteful consumption. Balancing explosive energy with rock properties and confinement conditions is crucial for efficient fragmentation and minimizing environmental impacts and structural damage. Environmental considerations are paramount since increased energy consumption may lead to higher greenhouse gas emissions, contributing to climate change. Exploring energy-efficient alternatives, such as advanced technologies, optimized drilling and blasting parameters, and alternative energy sources, is vital for reducing the environmental footprint of underground construction activities. In summary, energy consumption significantly influences underground construction processes involving rock breakers or blasting.

In addition, in underground engineering construction, the rocks exhibit varying energy absorption capacities, which are influenced by the impact energy levels. Consequently, this discrepancy in energy absorption leads to variations in energy consumption density. Furthermore, the extent of energy dissipation density directly impacts the degree of rock failure. Hence, it holds great importance to quantitatively assess the relationship between fractal dimensions and energy dissipation density in sandstones that possess diverse elastic velocities and water content. Figure 17 describes the correlation between fractal dimensions and energy dissipation density for the sandstones with diverse elastic velocities and water content. The figure indicates that the energy dissipation density and fractal size are essentially positively related. At a saturation of 0 and an impact velocity of 5 m/s, the energy dissipation density of sandstone is 1.06 and its fractal dimension is 1.99. At a saturation of 0 and an impact velocity of 10 m/s, the energy dissipation density of sandstone is 1.62 and its fractal dimension is 2.04. The findings indicate that there is a consistency between the evolution of fractal dimension and energy dissipation density. When the density of energy dissipation within the rock is large, the degree of rock fragmentation will inevitably increase in real-world engineering. Therefore, we should implement the appropriate prevention and control measures to limit the rate at which rock mass breaks.

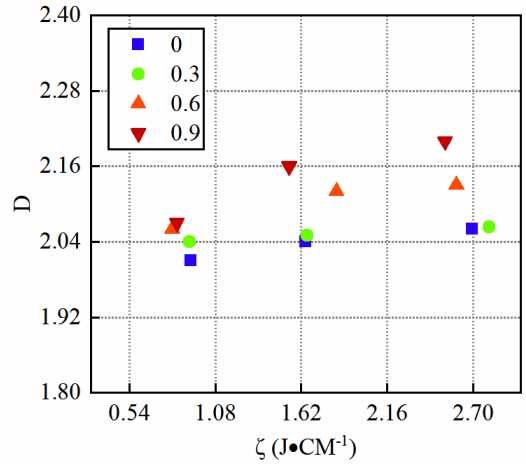

Figure 17. Correlation between samples' energy consumption density and fractal dimension.

4.7. Microscopic Fracture Mechanism

Upon exposure to water, the microstructure of rock undergoes notable transformations. Additionally, different bullet velocities lead to variations in the internal microstructure of the rock under loading conditions. Consequently, comprehending the microfracture mechanisms of rocks under the combined influence of dynamic loading and water is of utmost importance. Figure 18 presents the SEM analysis of rock micro-sections following failure under the coupled effects of dynamic loading and water. Trans-grain fractures (TG) and along grain fractures (IG) are represented in the analysis. The SEM images demonstrate characteristic features including pores, cracks, channels, and steps in the rocks after failure under the combined effects of dynamic loading and water. With increasing water content, the rock's porosity rises, and small pores tend to enlarge due to water infiltration, thereby augmenting the overall porosity. Lower water contents correspond to a relatively dense internal micro-particle arrangement within the rock. Conversely, higher water contents weaken the interparticle forces, resulting in a looser particle arrangement. This transformation occurs due to chemical interactions induced by water, leading to a transition from a compact to a loose internal structure. Moreover, Figure 19 illustrates the quantification of trans-grain fractures and along grain fractures, enabling an investigation into the microfracture mechanisms of sandstone under the combined effects of water and coupling. The presence of water significantly influences the ratio of trans-grain fractures to along grain fractures in the rock. Observing Figure 19, it becomes apparent that at lower

saturation levels, the rock's internal particles are primarily associated with trans-grain fractures, while along grain fractures play a secondary role. Conversely, at higher saturation levels, the rock's internal particles are predominantly associated with along grain fractures, with trans-grain fractures assuming a secondary role.

The SEM images reveal notable variations with increasing bullet velocity. As illustrated in Figures 20 and 21, lower bullet velocities predominantly exhibit along grain fractures within the rock's internal particles, accompanied by secondary trans-grain fractures. In contrast, higher bullet velocities demonstrate a shift towards trans-grain fractures as the primary mode, while along grain fractures assume a secondary role. It is worth noting that along grain fractures occur along crystal boundaries, resulting in crystal fracture, while trans-grain fractures transpire within the crystal structure itself. Notably, along grain fractures consume less energy due to their occurrence along crystal boundaries, whereas trans-grain fractures require more energy within the crystal structure. Consequently, rocks exhibit lower strength under along grain fractures and higher strength under trans-grain fractures at the macroscopic level. Thus, a microscopic analysis has been conducted to elucidate the strength mechanism of rocks under the coupled effects of dynamic loading and water.

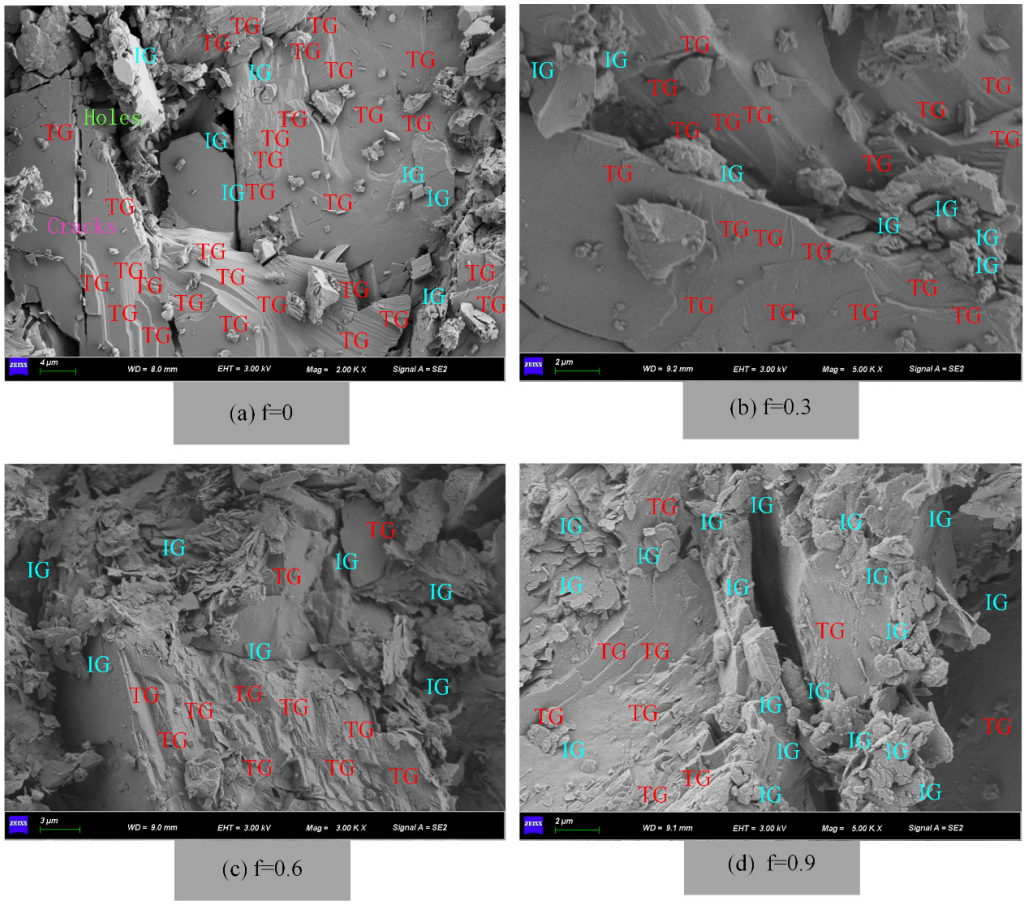

Figure 18. SEM image of sandstone at an impact velocity of 15 m/s.

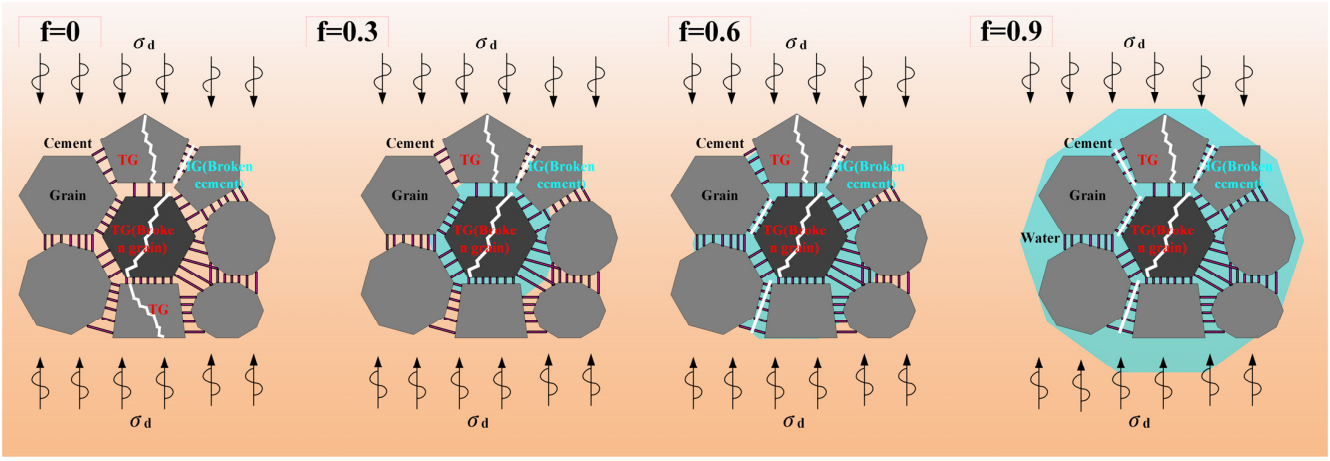

Figure 19. Illustration of the ratio between IG fractures and TG fractures in sandstone at an impact velocity of 15 m/s.

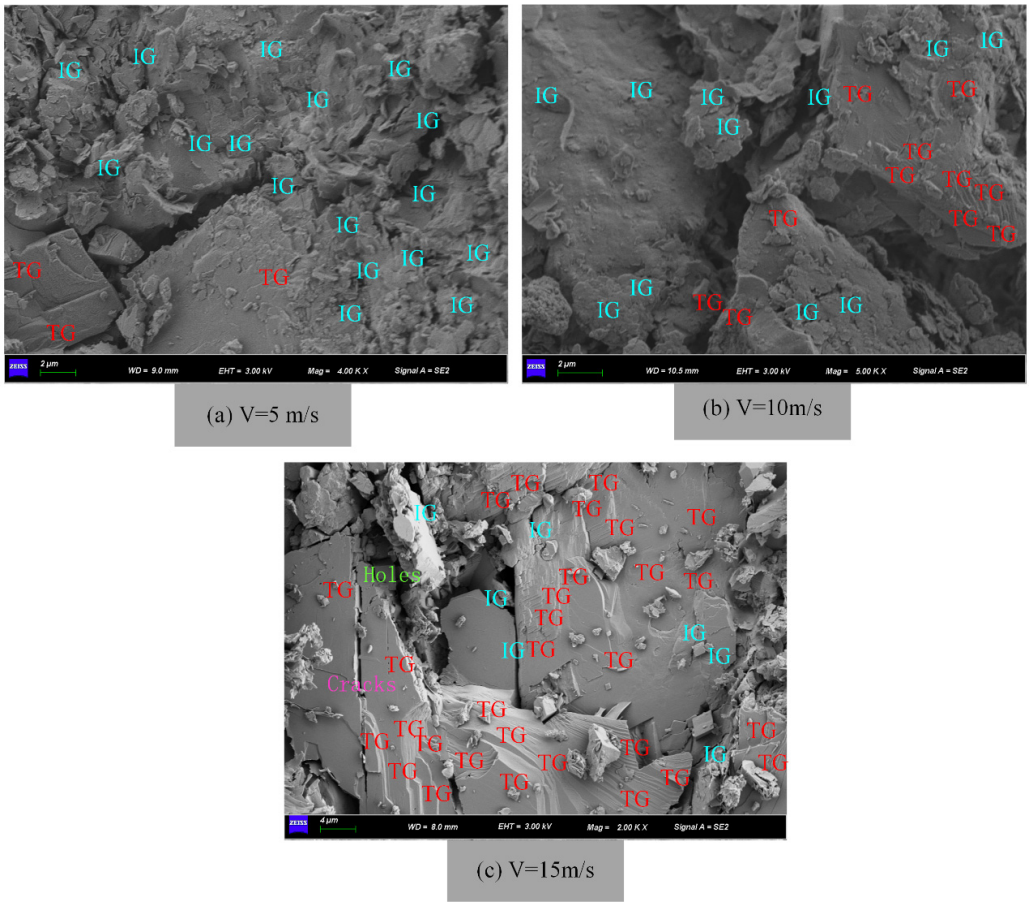

Figure 20. SEM image of sandstone at zero water saturation level.

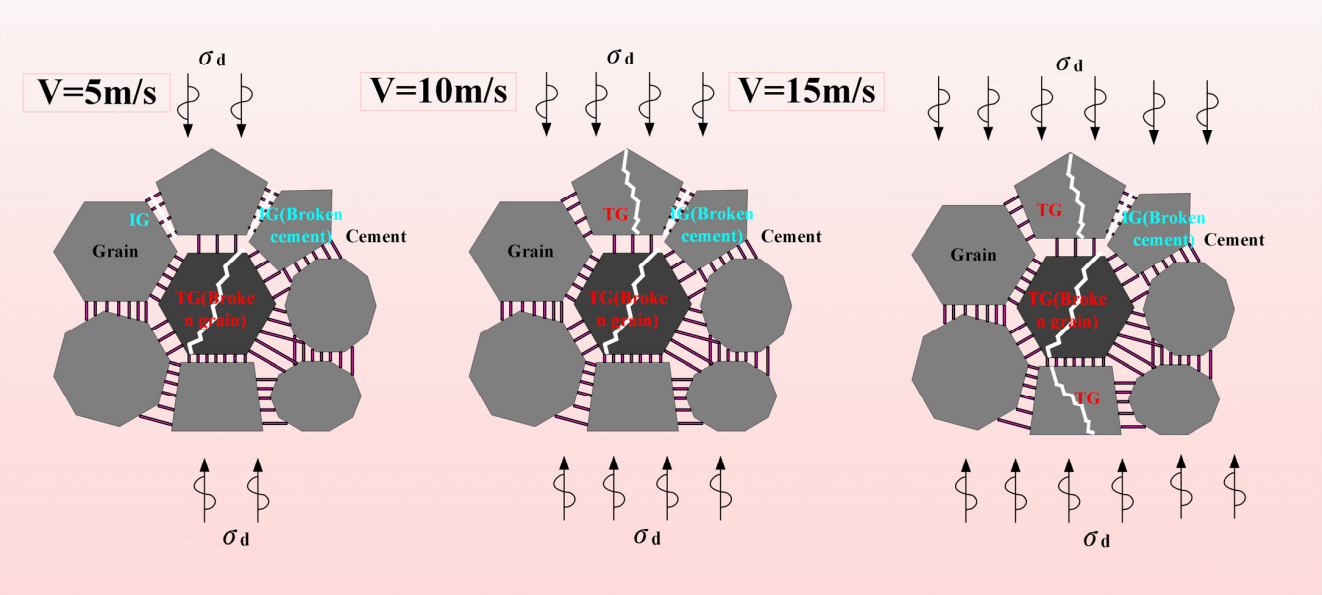

Figure 21. The schematic representation of the ratio between along grain fractures and trans-grain fractures in sandstone at zero water saturation level.

5. Conclusions

(1) Water content and bullet velocity significantly affect rock strength characteristics. Water content is negatively correlated with rock strength. Water weakens the rock's strength, while bullet velocity enhances the rock's strength. The peak strength of the rock increases as the velocity of the bullet rises.

(2) A novel approach was proposed to quantify along grain fractures and trans-grain fractures. It was found that as the bullet velocity increases, trans-grain fractures become dominant while along grain fractures play a secondary role. The presence of water also leads to changes in the microfracture mechanisms of rocks. Additionally, capillary forces, surface tension, and chemical reactions are equally significant factors contributing to the weakening of rock strength by water.

(3) Water content and bullet velocity significantly affect rock failure characteristics. The degree of sample fragmentation rises as the water content increases, and the fractal dimension as well. The mechanism of energy conversion in rock at varying water contents is very different.

(4) The density of energy dissipation has a major effect on the fractal dimension and peak strength of the rock. The density and intensity of energy dissipation and their fractal dimensions are quantified in this paper. It is observed that there is a positive relation between the intensity and density of energy dissipation. The higher the fractal dimension, the greater the rock's energy dissipation density and absorbed energy density.

Author Contributions: Y.C.: data curation; writing. T.K.: project administration. C.W.: formal analysis and investigation. All authors have read and agreed to the published version of the manuscript.

Funding: This research received no funding.

Data Availability Statement: The data that support the findings of this study are available from the corresponding author upon reasonable request.

Acknowledgments: The authors would like to thank shiyanjia lab (www.shiyanjia.com) for the support of SEM test.

Conflicts of Interest: The corresponding author declares no conflict of interest on behalf of all authors.

References

1. Zhu, W.; Li, S.; Niu, L.; Liu, K.; Xu, T. Experimental and Numerical Study on Stress Relaxation of Sandstones Disturbed by Dynamic Loading. *Rock Mech. Rock Eng.* **2016**, *49*, 3963–3982. [CrossRef]
2. Zhao, F.; Shi, Z.; Yu, S. Fracture mechanics behaviors of fissured rock under dynamic loading: A review. *Environ. Earth Sci.* **2022**, *81*, 526. [CrossRef]
3. Yang, S.; Yue, H.; Zhai, R.; Cui, Z.; Wei, X. 3D Physical Experimental Study of Shield–Strata Interaction Under Dynamic and Static Disturbance. *Front. Earth Sci.* **2022**, *10*, 913903. [CrossRef]
4. Wang, C.; Li, J.; Cheng, L.-P.; Li, X.-R.; Zhang, P.-L.; Hu, M.-G. Damage and Failure Characteristics and Constitutive Model of Copper-Bearing Skarns Disturbed by Hierarchical Dynamic Loading After Loading and Unloading. *Rock Mech. Rock Eng.* **2022**, *55*, 6981–7004. [CrossRef]
5. Chen, Q.; Zuo, Y.; Lin, J.; Chen, B.; Zheng, L. Numerical research on response characteristics of surrounding rock for deep layered clastic rock roadway under static and dynamic loading conditions. *Geomech. Geophys. Geo-Energy Geo-Resour.* **2022**, *8*, 91. [CrossRef]
6. Li, J.; Guo, P.; Cui, H.; Song, S.; Zhao, W.; Chu, J.; Xie, W. Dynamic Response Mechanism of Impact Instability Induced by Dynamic Load Disturbance to Surrounding Rock in High Static Loading Roadway. *Minerals* **2021**, *11*, 971. [CrossRef]
7. Shu, L.; Yuan, L.; Li, Q.; Xue, W.; Zhu, N.; Liu, Z. Response characteristics of gas pressure under simultaneous static and dynamic load: Implication for coal and gas outburst mechanism. *Int. J. Min. Sci. Technol.* **2023**, *33*, 155–171. [CrossRef]
8. Wang, C.; Cheng, L.P.; Wang, C.; Xiong, Z.Q.; Wei, S.M. Dynamic mechanical characteristics and failure mode of serpentine under a three-dimensional high static load and frequent dynamic disturbance. *PLoS ONE* **2019**, *14*, e0222684. [CrossRef]
9. Li, H.; Qiao, Y.; Shen, R.; He, M.; Cheng, T.; Xiao, Y.; Tang, J. Effect of water on mechanical behavior and acoustic emission response of sandstone during loading process: Phenomenon and mechanism. *Eng. Geol.* **2021**, *294*, 106386. [CrossRef]
10. Zhao, K.; Wang, X.; Wang, L.; Zeng, P.; Yang, D.; Jin, J. Investigation of the crack and acoustic emission behavior evolution of red sandstone subjected to water. *Theor. Appl. Fract. Mech.* **2022**, *120*, 103419. [CrossRef]
11. Luo, Y.; Wang, G.; Li, X.; Liu, T.; Mandal, A.K.; Xu, M.; Xu, K. Analysis of energy dissipation and crack evolution law of sandstone under impact load. *Int. J. Rock Mech. Min. Sci.* **2020**, *132*, 104359. [CrossRef]
12. Lu, A.; Chang, X.; Hu, S.; Xia, Y.; Li, M.; Zhang, H. Impact of Moisture Content on the Brittle-Ductile Transition and Microstructure of Sandstone under Dynamic Loading Conditions. *Adv. Civ. Eng.* **2021**, *2021*, 7644375. [CrossRef]
13. Gu, H.; Tao, M.; Li, X.; Cao, W.; Li, Q. Dynamic response and meso-deterioration mechanism of water-saturated sandstone under different porosities. *Measurement* **2021**, *167*, 108275. [CrossRef]
14. Yin, T.; Yin, J.; Wu, Y.; Yang, Z.; Liu, X.; Zhuang, D. Water saturation effects on the mechanical characteristics and fracture evolution of sandstone containing pre-existing flaws. *Theor. Appl. Fract. Mech.* **2022**, *122*, 103249. [CrossRef]
15. Kim, E.; Changani, H. Effect of water saturation and loading rate on the mechanical properties of Red and Buff Sandstones. *Int. J. Rock Mech. Min. Sci.* **2016**, *88*, 23–28. [CrossRef]
16. Li, M.; Lin, G.; Zhou, W.; Mao, X.; Zhang, L.; Mao, R. Experimental Study on Dynamic Tensile Failure of Sandstone Specimens with Different Water Contents. *Shock. Vib.* **2019**, *2019*, 7012752. [CrossRef]
17. Li, Y.; Wang, J. Effects of Porosity of Dry and Saturated Sandstone on the Energy Dissipation of Stress Wave. *Adv. Civ. Eng.* **2019**, *2019*, 9183969. [CrossRef]
18. Zhao, Y.; Yang, T.; Xu, T.; Zhang, P.; Shi, W. Mechanical and energy release characteristics of different water-bearing sandstones under uniaxial compression. *Int. J. Damage Mech.* **2017**, *27*, 640–656. [CrossRef]
19. Wang, P.; Yin, T.; Li, X.; Konietzky, H. Quasi-Static and Dynamic Tensile Behavior of Water-Bearing Sandstone Subjected to Microwave Irradiation. *Mathematics* **2022**, *11*, 203. [CrossRef]
20. Wang, P.; Yin, T.-B.; Hu, B.-W. Dynamic tensile strength and failure mechanisms of thermally treated sandstone under dry and water-saturated conditions. *Trans. Nonferrous Met. Soc. China* **2020**, *30*, 2217–2238. [CrossRef]
21. Niu, C.; Zhu, Z.; Wang, F.; Ying, P.; Deng, S. Effect of Water Content on Dynamic Fracture Characteristic of Rock under Impacts. *KSCE J. Civ. Eng.* **2020**, *25*, 37–50. [CrossRef]
22. Huang, S.; Yu, S. Effect of water saturation on the strength of sandstones: Experimental investigation and statistical analysis. *Bull. Eng. Geol. Environ.* **2022**, *81*, 323. [CrossRef]
23. Zhang, D.; Lu, G.; Wu, J.; Nie, W.; Ranjith, P.G. Effects of Ultralow Temperature and Water Saturation on the Mechanical Properties of Sandstone. *Rock Mech. Rock Eng.* **2023**, *56*, 3377–3397. [CrossRef]
24. Matejunas, A.; Tawney, J.; Reynolds, E.; Lamberson, L. Effects of Water Saturation on the Dynamic Compression and Fragmentation Response of Gabbroic Rock. *Rock Mech. Rock Eng.* **2022**, *55*, 4929–4939. [CrossRef]
25. Zhou, Z.; Yude, E.; Cai, X.; Zhang, J.; Xuan, D. Coupled Effects of Water and Low Temperature on Quasistatic and Dynamic Mechanical Behavior of Sandstone. *Geofluids* **2021**, *2021*, 9926063. [CrossRef]
26. Zhou, Z.; Cai, X.; Ma, D.; Du, X.; Chen, L.; Wang, H.; Zang, H. Water saturation effects on dynamic fracture behavior of sandstone. *Int. J. Rock Mech. Min. Sci.* **2019**, *114*, 46–61. [CrossRef]
27. Zhou, Z.; Cai, X.; Cao, W.; Li, X.; Xiong, C. Influence of Water Content on Mechanical Properties of Rock in Both Saturation and Drying Processes. *Rock Mech. Rock Eng.* **2016**, *49*, 3009–3025. [CrossRef]
28. Cai, X.; Zhou, Z.; Zang, H.; Song, Z. Water saturation effects on dynamic behavior and microstructure damage of sandstone: Phenomena and mechanisms. *Eng. Geol.* **2020**, *276*, 105760. [CrossRef]

29. Liu, J.; Xie, J.; Yang, B.; Li, F.; Deng, H.; Yang, Z.; Gao, M. Experimental Study on the Damage Characteristics and Acoustic Properties of Red Sandstone with Different Water Contents under Microwave Radiation. *Materials* **2023**, *16*, 979. [CrossRef]
30. Liu, X.; Dai, F.; Liu, Y.; Pei, P.; Yan, Z. Experimental Investigation of the Dynamic Tensile Properties of Naturally Saturated Rocks Using the Coupled Static–Dynamic Flattened Brazilian Disc Method. *Energies* **2021**, *14*, 4784. [CrossRef]
31. Ping, Q.; Gao, Q.; Wu, Y.; Wang, C.; Shen, K.; Wang, S.; Wu, S.; Xu, Y. Study on the Dynamic Splitting Mechanical Properties of Annular Sandstone Specimens with Temperature–Water Coupling in a Coal Mine. *Appl. Sci.* **2022**, *12*, 4608. [CrossRef]
32. Li, D.; Ma, J.; Zhu, Q.; Li, B. Research of Dynamic Tensile Properties of Five Rocks under Three Loading Modes Based on SHPB Device. *Materials* **2022**, *15*, 8473. [CrossRef] [PubMed]
33. Li, F.; Sun, R.; Zhang, Y.; Wang, G.; Xiang, G. Dynamic Response Characteristics and Damage Evolution of Multi-Layer Combined Coal and Rock Mass under Impact Loading. *Sustainability* **2022**, *14*, 9175. [CrossRef]
34. Li, Y.; Liu, J.; Yu, Q. Patterns of Influence of Parallel Rock Fractures on the Mechanical Properties of the Rock–Coal Combined Body. *Sustainability* **2022**, *14*, 13555. [CrossRef]
35. Chen, B.; Wang, L.; Zhang, M. Experimental Study of Confined-Pressure Soaking on Sandstone Damage-Fracture Characteristics Using Acoustic Emission and Energy Dissipation. *Sustainability* **2022**, *14*, 12381. [CrossRef]
36. Li, C.; Liu, N.; Liu, W.; Feng, R. Study on Characteristics of Energy Storage and Acoustic Emission of Rock under Different Moisture Content. *Sustainability* **2021**, *13*, 1041. [CrossRef]
37. Zhu, J.; Deng, J.; Chen, F.; Wang, F. Failure analysis of water-bearing rock under direct tension using acoustic emission. *Eng. Geol.* **2022**, *299*, 106541. [CrossRef]
38. Zhu, J.B.; Liao, Z.Y.; Tang, C.A. Numerical SHPB Tests of Rocks Under Combined Static and Dynamic Loading Conditions with Application to Dynamic Behavior of Rocks Under In Situ Stresses. *Rock Mech. Rock Eng.* **2016**, *49*, 3935–3946. [CrossRef]
39. Fan, W.; Zhang, J.; Dong, X.; Zhang, Y.; Yang, Y.; Zeng, W.; Wang, S. Fractal dimension and energy-damage evolution of deep-bedded sandstone under one-dimensional dynamic and static combined loading. *Geomech. Geophys. Geo-Energy Geo-Resour.* **2022**, *8*, 177. [CrossRef]
40. Dai, B.; Zhao, G.; Zhang, L.; Liu, Y.; Zhang, Z.; Luo, X.; Chen, Y. Energy Dissipation of Rock with Different Parallel Flaw Inclinations under Dynamic and Static Combined Loading. *Mathematics* **2022**, *10*, 4082. [CrossRef]